Mena Tobar, A.; Ferrero De Loma-Osorio, JM.; Migliavacca, F.; Rodríguez Matas, JF. (2018). Vulnerability in regionally ischemic human heart. Effect of the extracellular potassium concentration. Journal of Computational Science. 24:160-168. https://doi.org/10.1016/j.jocs.2017.11.009

Vulnerability in regionally ischemic human heart. Effect of the extracellular potassium concentration

Andrés Mena Tobar[a], José M. Ferrero[b], Francesco Migliavacca[c], José F. Rodríguez Matas[c,*]

[a] CIBER, Zaragoza, Spain
[b] Ci2B – Universitat Politecnica de Valencia, Valencia, Spain
[c] LabS, Department of Chemistry, Materials and Chemical Engineering "Giulio Natta", Politecnico di Milano, Milano, Italy

Keywords:
Acute ischemia
Numerical simulation
Vulnerable window
Wash-out zone

a b s t r a c t

Ventricular tachycardia and ventricular fibrillation are two types of cardiac arrhythmias that usually occur during acute ischemia and frequently lead to sudden death. Pro-arrhythmic mechanisms related to acute ischemia have been extensively investigated, although often in animal models rather than in human. In this work, we investigate how hyperkalemia affects the vulnerable window to reentry and the reentry patterns in the heterogeneous substrate caused by acute regional ischemia using an anatomically and biophysically detailed human biventricular model. The ischemic region was located in the inferolateral and posterior side of the left ventricle, mimicking the occlusion of the circumflex artery, and includes a wash-out zone not affected by ischemia located in the endocardium. Realistic heterogeneity and fiber anisotropy have been considered in the model. An electrophysiologically detailed human action potential model has been modified to simulate ischemic conditions. The model predicts the generation of sustained reentrant activity in the form of single and double circuits around an area of block within the ischemic zone for K^+ concentrations below 9 mM, with the reentrant activity corresponding to ventricular tachycardia in all cases. Our results also suggest that the wash-out zone is a potential pro-arrhythmic factor that favors sustained ventricular tachycardia.

1. Introduction

Ventricular tachycardia and fibrillation are known to be two types of cardiac arrhythmias that usually take place during acute ischemia, and frequently lead to sudden death [27]. Even though these arrhythmias arise from different conditions, ischemia is the most important perpetrator among them. The interruption of blood irrigation to the myocardium during acute ischemia has two main consequences from an electrophysiological point of view. Together with the reduction in nutrient delivery, the myocardium suffers a reduction in oxygen supply (hypoxia), an increase of extracellular potassium concentration $[K^+]_o$ (hyperkalemia), and an acidification of the underlying tissue (acidosis). These metabolic changes within the injured region cause significant alterations in the action potential (AP), a reduction in excitability and conduction velocity (CV), and an increase in the effective refractive period (ERP) among others [1,17]. In addition, these changes do not occur homogeneously within the injured region. In general, the impact of ischemia in the myocardium is characterised by a high degree of heterogeneity, both intramurally and transmurally, providing an important pro-arrhythmic substrate [3,15].

Pro-arrhythmic mechanisms of acute ischemia have been extensively investigated, although often in animal models rather than in human. Seminal studies by Janse et al. [16,17] in porcine and canine hearts highlight the complexity of the pro-arrhythmic and spatio-temporally dynamic substrate in acute ischemia. They observed that heterogeneity in excitability and repolarization properties across the borderzone leads to the establishment of reentry around the ischemic region after premature excitation [17,34]. The same studies also showed intramural reentry in certain cases, highlighting the potential variability in the mechanisms. However, the mechanisms that determine reentry formation and intramural patterns in acute ischemia in the three-dimensional human heart remain unclear, due to the low resolution of intramural recordings. In this regard, computer simulations of arrhythmias in three dimensional virtual human hearts may overcome these limitations and help to better understand the mechanisms of reentry initiation

* Corresponding author.
E-mail address: josefelix.rodriguezmatas@polimi.it (J.F. Rodríguez Matas).

and maintenance, as well as the interactions and synergies between the different scales.

In the past 20 years, mathematical modeling and computer simulations in electrophysiology have become a useful tool in analyzing myocardial arrhythmias [26]. In one of the first works on acute ischemia by Ferrero et al. [7], the authors analyze the role that metabolic changes produced during ischemia have on the electrophysiological behavior of cardiac tissue. However, these and subsequent simulations were limited to two dimensional tissue preparations [7,32], providing only a partial view of the problem. Three dimensional simulations have been limited to the globally ischemic heart [25], with limited work performed in modeling the human heart subjected to acute ischemic conditions [5,13,33]. In this regard, Weiss et al. [33], account for heterogeneities caused by ischemia, as well as AP duration (APD) differences, both transmurally and apex to base. However, their action potential under acute ischemic conditions used the model proposed by Ferrero et al. [6] for guinea pigs and did not report reentrant activity. Heidenreich et al. [13] developed a human acute ischemic heart accounting for realistic fiber orientation and transmural heterogeneities. Their model was able to predict the generation of non sustained reentry, which patterns were in partial agreement with those reported experimentally [15]. Dutta et al. [5] have investigated on how reduced repolarization increases arrhythmic risk in the heterogeneous substrate caused by acute myocardial ischemia. In their work, Dutta et al. [5] developed a human ventricular biophysically-detailed model with acute regional ischemia. Even tough macro-reentries around the ischemic zone were reported, these reentries self-terminated before completing three complete circuits, i.e., only non sustained reentry was achieved.

In this work, we investigate how hyperkalemia affects the vulnerable window to reentry and the reentry patterns in the heterogeneous substrate caused by acute regional ischemia, using an anatomically and biophysically detailed human biventricular model. This investigation develops on our previous model [13] based on the monodomain paradigm for simulating the propagation of APs in the heart. For the biophysical description of the AP under normal and ischemic conditions, the model proposed by ten Tusscher and Panfilov [30] (TP06) was used. In this regard, the model was modified to account for ischemia by incorporat- ing an ATP sensitive Potassium, IKATP, current. By analyzing high spatio-temporal resolution simulation data, we unravel the mech- anisms associated with the observed reentrant patterns observed in acutely-ischemic ventricles.

2. Methods

Simulation of the ischemic heart requires both an accurate description of the organ comprising its muscular structure and heterogeneity, and an appropriate model of its electrophysiologic behavior. The following sections offer a detailed description of the anatomical and biophysical model of the heart used in the present investigation, as well as the numerical methods used in the computations.

2.1. Heart model

The anatomically-based multiscale model of the heart relies on a previous model developed by our group [13]. Briefly, the geometry and fiber orientations were obtained from diffusion tensor magnetic resonance images (DT-MRI) acquired at John Hopkins University [14]. A regular volumetric mesh was constructed from the segmented images with hexahedral elements with a resolution of 0.4 mm × 0.4 mm × 0.4 mm, resulting in 1.43 million nodes and 1.29 million hexahedral elements.

Transmural heterogeneity of the electrophysiological properties across the heart is necessary to accurately describe normal cardiac function. In this regard, transmural differences in the electrophysiological behavior of the cells were introduced in order to obtain an APD gradient from the endocardium to the epicardium, with the longest APD at the midendocardium [11]. This was achieved by defining a layered distribution that includes the three cell types defined in the TP06 models in a proportion of 43% of epicardial cells, 20% of endocardial cells, and the remaining 37% being occupied by midmyocardial cells according to the APD distribution reported in [11] for the healthy human heart. This distribution resulted in a positive T wave in all synthetic electrograms computed in the precordial leads as shown in Fig. 1, in addition to a normal progression of the QRS complex (for the case of acute ischemia under investigation). As in other works [5,13], the present model does not incorporate explicit apex-to-base APD heterogeneity.

2.2. Action potential model under ischemic conditions

All simulations were performed with a modified version of the ten Tusscher and Panfilov (TP06) model of the human AP [30]. The model describes with high degree of electrophysiological detail the principal transmembrane ionic currents: sodium current I_{Na}, L-type calcium current I_{CaL}, inward rectifying current I_{K1}, fast delayed rectifying current I_{Kr}, slow delayed rectifying current I_{Ks}, tran- sient outward current I_{to}, sodium–calcium exchanger current I_{NaCa}, sodium–potassium pump current I_{NaK}, plateau calcium and potassium currents I_{pCa} and I_{pK} respectively, and background sodium and calcium currents I_{bNa} and I_{bCa}. In order to describe the electrophysiological changes caused by ischemia, the model was provided with a modified formulation of the ATP-sensitive K^+ current (I_{KATP}) proposed by Ferrero et al. [6]. The methodology was explained in detail in our previous work [13]. Briefly, the I_{KATP} current was formulated as

$$I_{KATP} = g_0 \left(\frac{[K_o^+]}{5.4} \right)^{0.24} f_M f_N f_T f_{ATP} (V - E_K),$$

where g_0 is the maximum channel conductance in the absence of Na^+, Mg^{2+} and ATP; f_M, f_N, f_T are inward-rectification-related factors given in [6] that we kept unaltered in the modified model; f_{ATP} is the fraction of open channels; V is the transmembrane potential; and E_K is the reversal potential of the channel (Nernst potential). The fraction of open channels, f_{ATP}, is given by [13]

$$f_{ATP} = \frac{1}{1 + ([ATP]_i / K_m)^H},$$

where $[ATP]_i$ is the ATP intracellular concentration in mmol/L, with K_m (in mmol/L) and H (–) given by

$$K_m = (35.8 + 17.9[ADP]_i^{0.256}, \quad (3)$$

$$H = 1.3 + 4.44 \exp(-0.09[ADP]_i), \quad (4)$$

where $[ADP]_i$ is the intracellular concentration of ADP in μmol/L, and a parameter that accounts for cellular heterogeneity. Parameter was identified by fitting experimental data available for different animal models and cell types (see Fig. 2.2 in [13]) in addition to human data reported in Koumi et al. [20]. This approach has been adopted by others when developing an heterogeneous model of I_{KATP} [10,22]. Due to the absence of experimental data, our model of the ATP influence in the fraction of open channels in midmyocardial cells assumes a value of , that yields the same percentage reduction in APD as in endocardial cells. This decision was taken based on the results from Wilensky et al. [34] who found a 40% reduction in APD for cells 1 mm deep from the endocardial surface in the case of phase 1a ischemia (10 min after coronary occlusion).

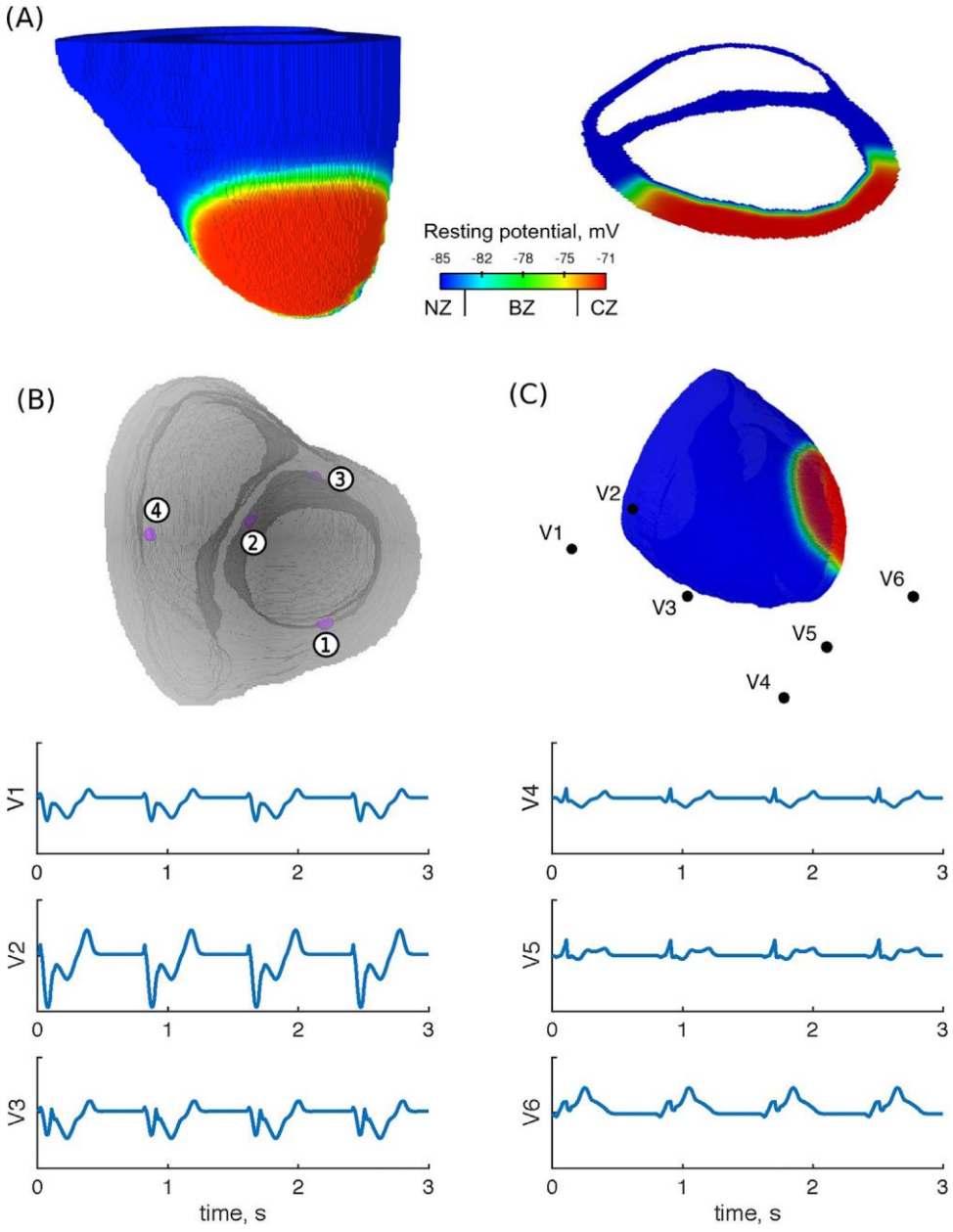

Fig. 1. Electrophysiological heterogeneity in the acute regional ischemic heart. (A) Resting potential in the heterogeneous heart showing higher transmembrane potential in the ischemic tissue (CZ) and the transition through the border zone (BZ). The right panel shows a detail of the washed-zone at the endocardium defined in the model as reported in [34]. (B) Stimulation sites for the normal SA stimulation according to [4]. (C) Location of the pseudo-ECG probes corresponding to the six leads of the standard ECG. A pseudo-ECG is depicted in the bottom panel, exhibiting the ST elevation in V5–V6, with an acute T-wave in V6, and ST depression in V1–V4 consistent with an infarction involving the inferior, lateral and posterior walls caused by the occlusion of the proximal circumflex artery. In addition, the positive T wave following the changes in the ST segment is consistent with the inverse relationship between APD and activation times.

Differently to our previous work [13], parameter g_0 was identified for the epicardial cells first and then this value was used for the remaining cell types. We then verified that the modified AP model for the other cells was able to reproduce the changes in APD for ischemic conditions. We adopted this strategy as we believed it was reasonable to assume the maximal channel conductance g_0 to be independent of the cell type. To test the model, 100 stimuli at a basic cycle length (BCL) of 1000 ms were applied to an isolated cell. The APD at the last stimulus was measured under physiological and pathological conditions. Table 1 shows the adopted $[K^+]_o$, $[ATP]_i$ and $[ADP]_i$ values to define physiological and ischemic conditions. Table 2 summarizes the parameters used in the I_{KATP} current model. The table also shows the value of APD computed for the physiological and ischemic conditions defined in Table 1. The value of APD obtained when the I_{KATP} current remains inactive is also shown for completeness.

Table 1
Extracellular potassium and intracellular ADP and ATP concentrations defining physiological and ischemic conditions for the simulations.

Condition	$[K^+]_o$ mM	$[ATP]_i$ mM	$[ADP]_i$ μM
Normoxia	5.4	6.8	15.0
Ischemia	9.9	4.6	99.0

The APD variation between normal and hypoxic conditions given in Table 2 are in good agreement with experimental observations by Furukawa et al. [8]. Additional tests were conducted in a one-dimensional cable in order to assess the effect of electrotonic

Table 2
Value of the parameters for the I_{KATP} current adapted to the ten Tusscher model for different cell types. Also shown, the computed APD for the physiological and ischemic conditions in Table 1, and the APD associated with the original TP06 model.

Cell	Parameter		I_{KATP} active		I_{KATP} inactive
Type	g_0	-	APD_{90}^{Nor}	APD_{90}^{Isq}	APD_{90}^{Nor}
	mS	–	ms	ms	ms
ENDO	4.5	0.32	299	265	299
MID	4.5	0.86	393	178	393
EPI	4.5	1.0	298	141	298

coupling. We found that electrotonic coupling reduced APD in less than 1%, in good agreement with results reported elsewhere [2]. In addition, the percentage reduction in APD between physiological and ischemic conditions shown in Table 2 were maintained.

2.3. Electrophysiological heterogeneities under acute ischemia

The ischemic region was located in the inferolateral and posterior side of the left ventricle, mimicking the occlusion of the circumflex coronary artery (see Fig. 1A). The ischemic region comprised realistically dimensioned transitional border zones (BZ), a normal zone (NZ), and the ischemic central zone (CZ), mimicking experimental findings [3] during the early stages of ischemia. In order to study three different time frames during acute ischemia, $[K^+]_o$ was set at three different values (7.0, 8.0 and 9.0 mM) in the CZ. The inward Na^+ and L-type Ca^{2+} currents were scaled by a factor of 0.85 to mimic the effect of acidosis [7,35], whereas $[ATP]_i$ and $[ADP]_i$ concentrations were set to 5 mM and 99 μM respectively [16]. The border zone included a linear variation in the electrophysiological properties between the NZ and the IZ as shown in experiments [3]. In addition, the model includes a 1.0 mm washout zone (not affected by ischemia) in the endocardium (see right panel in Fig. 1A), which results from the interaction between the endocardial tissue and the blood in the ventricular cavities (Wilensky et al. [34]). The resulting human ventricular model in acute regional ischemia produced correct synthetic electrocardiograms at the six precordial leads (see bottom panel in Fig. 1), exhibiting the ST elevation in V5–V6, with an acute T-wave in V6, and ST depression in V1–V4, consistent with an acute myocardial infarction involving the inferior, lateral and posterior walls caused by the occlusion of the proximal circumflex artery [23].

2.4. Stimulation protocol

Our model does not incorporate the specialized conduction system of the heart. However, Purkinje-like stimulation was simulated by stimulating discrete zones of the endocardium according to the results reported by Durrer et al. [4], an approach followed by others [5,13]. According to Durrer et al. [4], endocardial stimulation in the left ventricle starts at three well-defined locations within a time window of 5 ms: (i) An area on the superior anterior paraseptal wall just below the attachment of the mitral valve; (ii) A central area on the left surface of the interventricular septum; and (iii) The posterior paraseptal area at about one third of the distance from apex to base. For the right ventricle, we have defined a stimulation area near the insertion of the anterior papillary muscle. In the right ventricle, stimulation starts 5 ms after the onset of the left ventricular propagation [4]. Fig. 1B shows the location for the four stimulation areas.

The model was preconditioned with endocardial stimulation (S1) consisting on 56 stimuli delivered at a cycle length (CL) of 800 ms (frequency of 1.25 Hz). Following the preconditioning, an extra-stimulus, or premature stimulation, (S2) was applied in the subendocardial border zone in agreement with [16]. The coupling interval (CI), e.g., the time difference between S1 and S2, was varied with a resolution of 1 ms to determine the vulnerable window of reentry. A depolarization pattern was considered as a reentry if at least two cycles were completed around the ischemic zone. Sustained reentrant patterns were studied during three seconds after the extra stimulus for different values of extracellular potassium concentration in the CZ.

2.5. Numerical methods

The variation of the transmembrane potential, V, in the heart was modeled using the monodomain model [9]

$$\nabla \cdot (\mathbf{D}\nabla V) = C_m \frac{\partial V}{\partial t} + J_{ion}(V, \mathbf{w}) + J_{stm},$$

$$\frac{\partial \mathbf{w}}{\partial t} = \mathbf{f}(\mathbf{w}, V, t),$$

where $\mathbf{D}$ is the symmetric and positive definite conductivity tensor, C_m the membrane capacitance, $J_{ion}(V, \mathbf{w})$ the transmembrane ionic current, J_{stm} the stimulation current, $\mathbf{w}$ is a vector of gating variables and concentrations, $\mathbf{f}$ is a vector valued function, and t is time. Both, J_{ion} and $\mathbf{f}$ depend on the cellular model used. The TP06 ionic model includes 13 gating variables and 5 ionic concentrations for a total of 19 state variables (including V).

The boundary conditions associated with the monodomain model are

$$\mathbf{n} \cdot \nabla (\mathbf{D} \nabla V) = 0. \tag{7}$$

where $\mathbf{n}$ is the outward normal.

The tissue was assumed to be transversally isotropic with $\mathbf{D}$ defined as

$$\mathbf{D} = a_L[(1 - r)\mathbf{n}_f \otimes \mathbf{n}_f + r\mathbf{I}], \tag{8}$$

where $\mathbf{n}_f$ is the local muscle fiber direction, a_L is the conductivity of the tissue along the fiber, $r = a_T/a_L$ with a_T the conductivity in the direction perpendicular to the fiber, and $\mathbf{I}$ is the second order identity tensor. For the simulations we set $a_L = 0.00132$ cm^2/ms and $r = 0.475$ which led to a maximum planar conduction velocity of 66 cm/s along the fiber direction and 39 cm/s perpendicular to the fiber direction in good agreement with experiments in human myocardium [4,29]. Calibration of the conduction velocity was performed on a prism 2 cm × 2 cm × 10 cm by delivering a planar wave along the longest axes of the prism and measuring the conduction velocity in the middle of the prism. In addition, the membrane capacitance has been set to 1 μF/cm^2.

The monodomain model represents an important simplification of the more complex bidomain model [9], but offers important advantages for mathematical analysis and computation. Despite its simplicity, this model is adequate for studying a number of electrophysiological problems as ventricular fibrillation or the onset of ischemia in the electric behavior of the heart [7,5,30]. From a mathematical and numerical point of view, Eqs. (5)–(7) represent a reaction-diffusion equation. This problem was solved using the finite element method for spatial discretization, in conjunction with the operator splitting scheme in combination with the implicit Euler method for the time discretization, as described in [12,21]. Computations were performed with the GPU-based software TOR [21] using a fixed time step of 0.02 ms. Simulation of 1 s of electric activity took 1.5 h on a GPU Tesla M2090 (6GRAM DDR5).

Assuming that the heart is immersed in an infinite homogeneous isotropic medium, synthetic electrograms (pseudo-ECGs) were obtained using the transmembrane membrane potential, V,

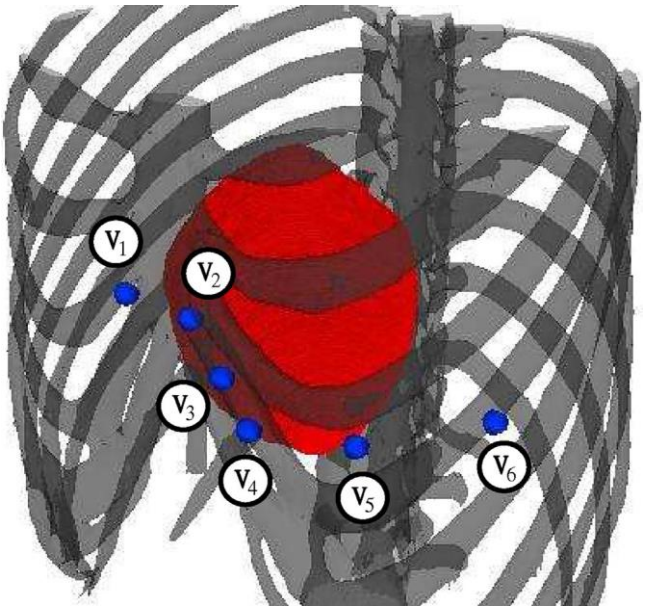

Fig. 2. Segmented torso with the heart model used on this investigation along with the location of the precordial leads used to compute the pseudo-ECG.

in all nodes of the heart mesh [9,24]. Specifically, the surface electrocardiogram in the ith lead, $cf>_i$, was obtained as:

$$\Phi_i = -\int_{\mathcal{H}} \sigma \nabla V \cdot \nabla \left(\frac{1}{d}\right) \mathrm{d}v,$$

where a is a constant associated to the conductivity of the extracellular medium, d the distance between the electrode and dv, and H is the domain of integration (i.e., the ventricular volume).

The pseudo-ECG was computed in six different positions that correspond with the precordial leads as shown in Fig. 1C. In order to correctly locate the position of the electrodes, we positioned our model of the heart in a segmented torso in place of the original heart. The position of the electrodes corresponded to the location of the six precordial lead electrodes. The torso dataset was obtained from the online open repository at the Centre for Integrative Biomedical Computing (CBIC) from University of Utah [31]. Data in this repository was anonymised and open to the research community at the time of building the new 3D torso model (RIUNET, http://hdl.handle.net/10251/55150). The bones and ventricles present in the torso were reconstructed by grey-level threshold segmentation by means of the software Mimics (The Materialise Group, Leuven, Belgium). Fig. 2 shows the segmented torso with the heart model positioned in the thorax along with the location of the six precordial leads.

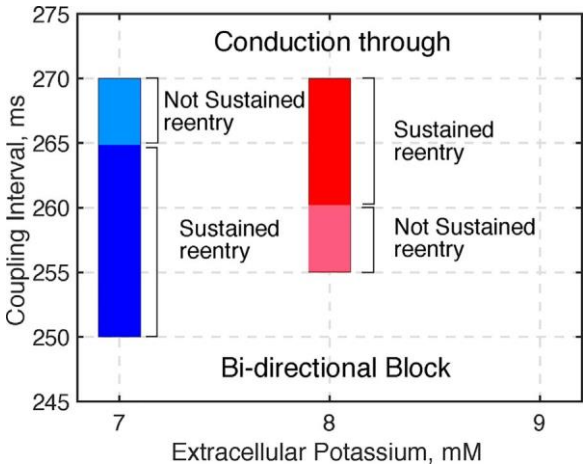

Fig. 4. Vulnerable window for different levels of $[K^+]_o$. Early stimulation starts at point F in Fig. 3.

3. Results

In general, our results show spatial heterogeneities in the propagated action potential throughout the regional ischemic tissue, as reported experimentally, such as in resting membrane potential (–85.2 mV in the NZ, and–72.5 mV in the CZ, with potentials varying between these values in the BZ). During a basic beat, activity spreads from three directions into the ischemic area as shown in Fig. 3A. A premature stimulus was delivered at the point of first activation in the subendocardium of the BZ after the last the basic beat (see point F in Fig. 3B).

The premature stimulus was delivered at different coupling intervals to determine the vulnerable window for three different levels of extracellular potassium, $[K^+]_o$. Fig. 4 shows the results for an early activation initiating at point F in Fig. 3.

Extracellular potassium concentration was found to have a significant effect on the size of the vulnerable window. For $[K^+]_o$ = 7 mM, the vulnerable windows was found to be the largest (20 ms), with CIs originating reentry between 250 and 270 ms. For CIs between 250 and 265 ms, sustained reentry (lasting more that 3 s, about 7–8 beats) was observed, whereas for CIs between 265 and 270, the reentrant activity self-terminated after three reentry circuits (3 beats). For $[K^+]_o$=8 mM the vulnerable window was reduced to 15 ms (CIs between 255 and 270 ms). In this case,

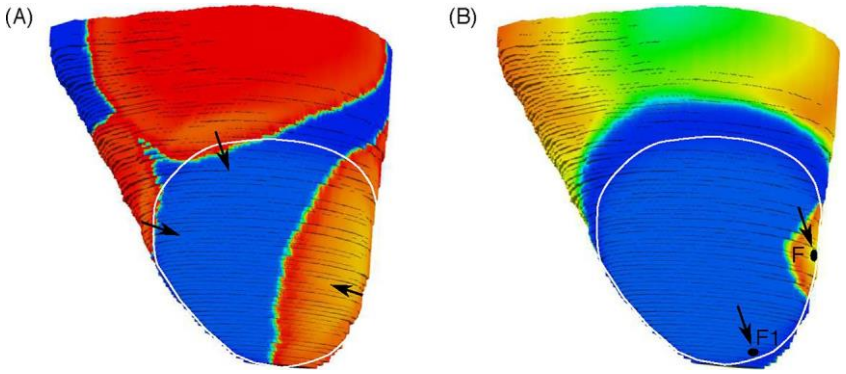

Fig. 3. Depolarization pattern through the ischemic tissue (delimited by the white line) during basic activation (A), and right after the premature stimulus (B). The ischemic tissue is depolarized by three different fronts coming from the normal activation sites shown in Fig. 1B. The ectopic beat was delivered at the subendocardium of first point being depolarized within the ischemic tissue (point F in the right panel).

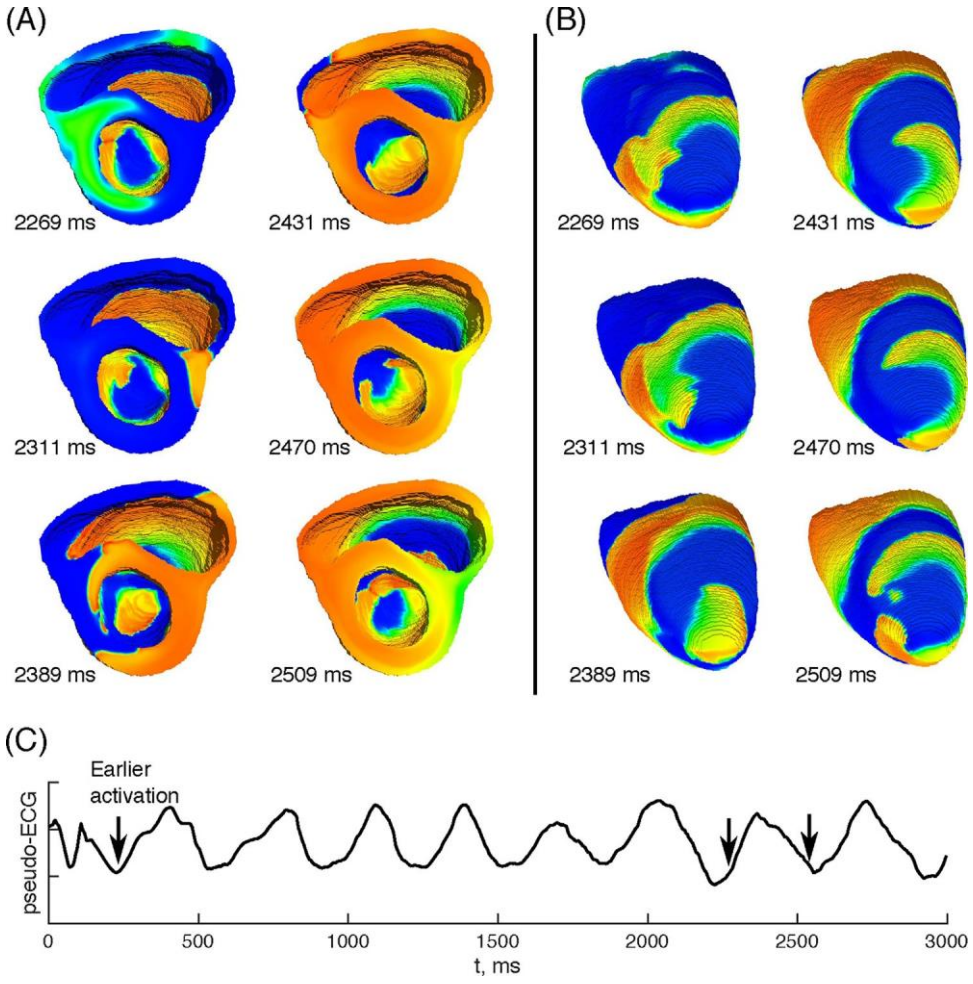

Fig. 5. Reentrant patterns at endocardium (A) and epicardium (B) for the last recorded beat for the case $[K^+]_o$ = 7.0 mM and CI = 260 ms. Panel C shows the pseudo-ECG corresponding to the lead V3, the arrows indicate the window corresponding to the patterns shown in panels (A) and (B).

sustained reentry was observed for CIs between 255 and 265 ms. Conversely, no reentrant activity was found for $[K^+]_o$ = 9.0 mM. In general, for CIs below the lower limit of the vulnerable window, bidirectional block occurred without generating re-entrant activity. Conversely, for CIs above the upper limit of the vulnerable window, conduction through the ischemic zone occurred.

Fig. 4 shows that the results depend on the location of the premature stimulation. To explore this fact, the vulnerable window was determined for point *F*1 in Fig. 3. As in the previous case, no-reentrant activity was obtained for $[K^+]_o$ = 9.0 mM. For $[K^+]_o$ = 7.0 mM, the vulnerable window reduced to 10 ms (CI between 265 and 275 ms) with the reentrant activity self-terminating after two beats (800 ms). A similar result was obtained for the case of $[K^+]_o$ = 8.0 mM, with reentrant activity observed for CIs between 290 and 310 ms that self-terminated after two reentrant circuits.

The reentrant activity observed for different levels of $[K^+]_o$, and different prematurely stimulated sites, mimicked ventricular tachycardia in all cases without degeneration in ventricular fibrillation, at least within the observed window of 3 seconds after earlier stimulation (see Fig. 5). In all cases where sustained reentry was found, the same pattern emerged at the epicardium. After initiating early activity (at point *F* in Fig. 3), conduction within the ischemic region slows down (see the frequency of the pseudo-ECG in Fig. 5C) and a fragmented wavefront with multiple areas of conduction block are observed in the epicardium due to intramural reentry (see bellow). In subsequent beats, this pattern evolves into a circus, or double circus, movement within the CZ around an area with a diameter of around 4.0 cm and a period in the order of 250 ms as shown in Fig. 5B for the last recorded beat ($[K^+]_o$ = 7.0 mM and CI = 260 ms).

Detailed observation of the activation activity at the endocardium in Fig. 5A reveals a faster circus movement in the endocardium as compared to the epicardium, with a period in the order of 200 ms. This behavior is due to the presence of the wash-out zone that allows faster conduction velocity. Also, the fragmentation of the wavefront at the epicardium appears to be related to the presence of the wash-out zone since it favors transmural reentry. Fig. 6A shows a snapshot of the transmembrane potential at the epicardium and endocardium at t = 2500 ms after initiation of earlier stimulation (last recorded beat) for a $[K^+]_o$ = 7.0 mM and CI = 260 ms. The figure demonstrates how the double circuit closes first at the endocardium. The transmural map of the transmembrane potential depicted in Fig. 6B shows how the faster endocardial conduction favors intramural conduction, causing this wavefront to emerge at the epicardium at t = 2509 ms as shown in Fig. 5B.

Even though basically one circus movement of relatively large dimensions is the responsible for the sustained tachycardia, the pattern of the reentrant wavefront, position and dimensions changes from beat to beat. Fig. 7 shows the changes in the pattern from a single circuit to a double circuit in the form of a figure-of-eight reentry, for the case of $[K^+]_o$ = 7.0 mM and CI = 260 ms. The reentry was always observed within the ischemic region. In addition, in all cases where sustained reentry was found, the reentrant

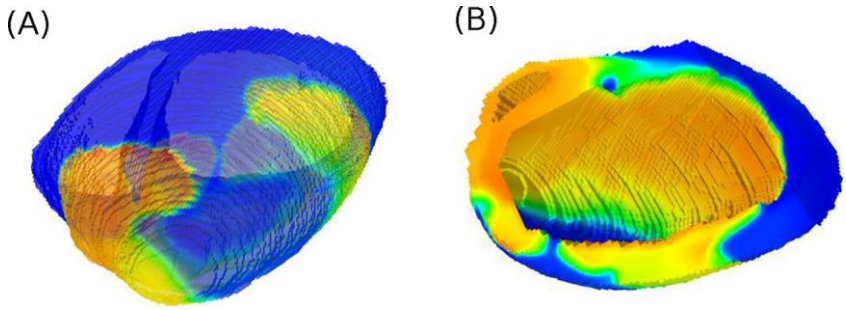

Fig. 6. Transmembrane potential at t = 2500 ms after initiation of earlier stimulation ($[K^+]_o$ = 7.0 mM and CI = 260 ms). (A) Depolarization map at the epicardium and endocardium. (B) Transmural depolarization map.

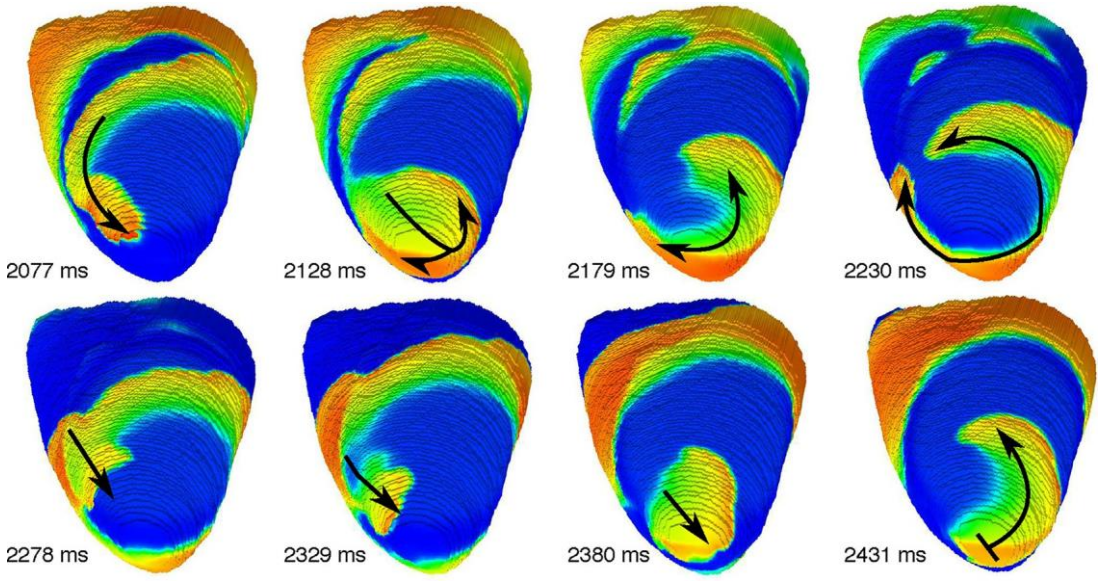

Fig. 7. Evolution of the reentry pattern from beat to beat. The sequence indicates an evolution from a single circus to a double circus (figure of eight) to then come back to a single circus patter ($[K^+]_o$ = 7.0 mM and CI = 260 ms).

front was lead from the endocardial surface where the pattern was clearly identified for all CIs. Reentry patterns were not altered when the basic stimulation was maintained after delivering the extra-stimulus, indicating that tachycardia overrides normal stimulation.

Our results also indicate that reentrant activity may be sustained in part by the presence of a wash-out zone in the endocardium as suggested by Wilensky et al. [34]. In order to get a better insight, all simulations were repeated with a heart model without the wash-out zone. Fig. 8 shows the vulnerable window for the model without wash-out zone for a premature stimulation delivered at point *F* in Fig. 3. The most significant finding was that all reentries self-terminated after two or three complete circuits. The model without wash-out zone still predicts non sustained reentries for $[K^+]_o$ = 7 mN and $[K^+]_o$ = 8 mN, but for a much reduced vulnerable window as compared to the model with the wash-out zone. In addition, non sustained reentries were found for $[K^+]_o$ = 9 mM for CIs between 310 ms and 370 ms.

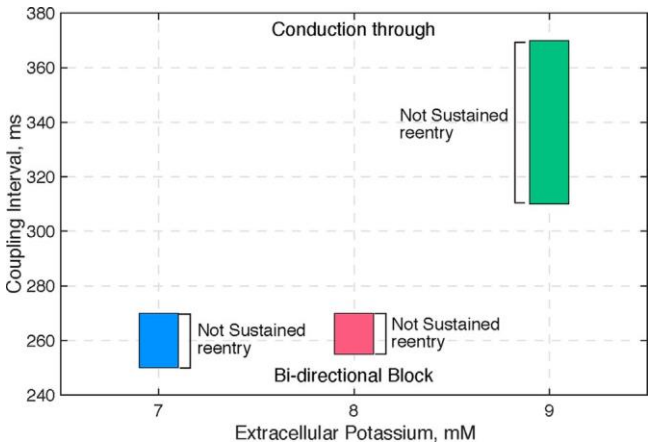

Fig. 8. Vulnerable window for different levels of $[K^+]_o$ in a model without the washed-out zone. Early stimulation starts at point F in Fig. 3.

4. Discussion

We have developed a biventricular human model that combines a realistic anatomy and actual fiber orientations obtained from MR-DTI. In addition, the model integrates the biophysical features of membrane kinetics, as well as the electrophysiological alterations induced by acute regional ischemia. In this regard, the size of the ischemic area was defined according to previous studies [3]. In spite of a lack of a specialized conduction system, our simulation results are in agreement with experimental studies and clinical observations [18]. Ventricular activation is in agreement with results from Durrer et al. [4]. Pseudo-ECGs at the six precordial leads (see bottom panel in Fig. 1) are consistent with an acute myocardial infarction caused by the occlusion of the proximal circumflex artery [23].

Extracellular potassium concentration $[K^+]_o$, the factor that most influences the effective refractive period (ERP) in single cell kinetics [7,6], has also a significant effect on the vulnerable window. We found that the size of the vulnerable window decreases as $[K^+]_o$ increases. Even though we did not perform simulations for lower values of $[K^+]_o$ than 7 mM, these results are in agreement with the experimental findings from Smith et al. [28] that reported that the peak of arrhythmic events during the phase 1a acute regional ischemia occurs between the first five to nine minutes after occlusion. For this time window, Coronel et al. [3] reported that the accumulation of $[K^+]_o$ in the CZ rises from 6 mM to 8.5 mM. A possible explanation for this behavior lies on the relationship between the ERP and $[K^+]_o$. As $[K^+]_o$ increases, ERP also increases, thus reducing the likelihood of reentry if the size of the ischemic area remains unaltered. In other words, a prolonged ERP in ischemic tissue would require either an increase in the size of the ischemic region or a decrease conduction velocity. The size of the ischemic region is defined by the occluded vessel and remains unchanged while local changes in $[K^+]_o$, $[ATP]_i$, $[ADP]_i$, and PH occur, as demonstrated by a number of studies [3,16,28,34]. In addition, Smith et al. [28] show that there is a relatively small increase in tissue resistivity during the first 10 min of ischemia (in the order of 30–50% of initial values). However, after 15 min of ischemia (phase 1b ischemia), a more prominent rise in tissue resistivity begins to develop due to progressive cell-to-cell electrical uncoupling. Electrical uncoupling implies a significant reduction in conduction velocity, favoring the development of reentry activity.

The macro-reentrant patterns of activation obtained in the regionally ischemic human biventricular model are consistent with those reported by Janse et al. [16] in porcine and canine hearts. In all our simulations, reentrant activity corresponded to ventricular tachycardia without registering ventricular fibrillation episodes. This is also in agreement with experiments from Smith et al. [28] which reported the onset of ventricular fibrillation to be cluster between 19 and 30 min of ischemia corresponding to the 1b phase. After stabilization of the reentrant activity, one circuit (single rotor) of fairly large dimension was basically observed with the activity circling around an area of block with a size equivalent to the CZ. For some beats, double circuits were observed but not sustained, and the reentrant activity continued because of one single reentrant circuit. Patterns from our simulations closely resemble those reported by Janse et al. [16]. For instance, Fig. 8 in [16] shows a single circuit and a figure-of-eight pattern, similar to those observed in our simulations (see Fig. 7).

The presence of a wash-out zone in the endocardium of the biophysical model of the heart has been determinant in the development of sustained reentry. The explanation of the observed differences in the vulnerable window between the model with and without wash-out zone was found in the rapid increase in the ERP as $[K^+]_o$ increases. For lower concentrations, the lower conduction velocity in the endocardium in the model without wash-out zone significantly reduces the time window for which reentrant activity can be established. Conversely, as potassium concentration increases, e.g., $[K^+]_o$=9 mM, the slower conduction velocity associated with the ischemic tissue in the endocardium allows to close the reentrant circuit which otherwise would find the tissue within the refractory period as happened in the model with the wash-out zone.

A number of limitations are present in this study. The Purkinje system was not present in our model since we were interested in studying the mechanisms associated with reentry rather than the biophysical mechanisms leading to ectopic excitation. In this regard, the study by Janse et al. [16] suggests that earlier activation is most likely due to focal activity localized in the Purkinje fibers close to the ischemic border zone. Future studies, however, are intended to extend our study to evaluate the implication of the Purkinje system in earlier activation during acute regional ischemia and its potential role in contributing to arrhythmogenesis. However, a recent study by Dutta et al. [5] suggests that early activation causing transmural micro-reentry could be generated by electrotonically-triggered EADs at the endocardium.

A second important limitation is related to the definition of the ischemic zone itself. We have considered an idealized shape with smooth borders and transitions between the CZ and the NZ. Patient specific acute regional ischemic areas are expected to have tortuous borders that may contribute to modify the evolution of the reentry patterns and the vulnerable window. However, we believe that the general patterns that have emerged in this study will not be significantly modified by the actual shape of the ischemic area as long as the general dimensions of the ischemic zone are maintained. In addition, we have only monitored the reentrant activity up to three seconds during which we have observed perpetuating activity for a restricted vulnerable window. In some cases, i.e., CI between 265 ms and 270 ms for $[K^+]_o$ = 7.0 mM, the reentrant activity spontaneously terminated after completing three reentrant circuits. This type of behavior was also reported in [16] where tachycardia terminated within 30 s after initiation. Additional studies on larger ischemic zones are required in order to determine if the size of the ischemic area may favor the onset of ventricular fibrillation in the ischemic heart. In addition, the location of the ectopic activity is important for both the size of the vulnerable window and the reentrant pattern.

Finally, our model only includes transmural heterogeneity, neglecting the apex-to-base dispersion in the APD. This approximation was also followed by Dutta et al. [5]. The decision of not accounting for this heterogeneity could be justified by the differences between the transmural and the apex-to-base APD gradients. Apex-to base dispersion of the APD is of the order of 25 ms versus 16 ms endo–epi (even though this is not linear) [19,33]. Taking into account the dimensions of the heart implies that, the approximate apex-to-base APD gradient is of the order of 5 ms/cm versus an approximate 20 ms/cm endo–epi, a fourfold difference.

In conclusion, the model predicts the generation of reentry within the ischemic zone due to the heterogeneity in the refractory period between the area affected by ischemia and the normal myocardium. The patterns obtained with the simulations are in good agreement with experimental studies conducted in porcine and canine hearts subject to acute regional ischemia. The main results of the simulations can be summarized as follows: (i) As a consequence of the applied premature extra-stimulus, reentrant activity generated for CIs which range depends on the value of the extracellular potassium concentration $[K^+]_o$; (ii) The reentrant activity generated due to the extra-stimulus was initiated as a consequence of the interaction between wavefronts emerging from the wash-out zone into the ischemic zone; (iii) results suggest that the wash-out zone could act as a pro-arrhythmic substrate helping on establishing sustained ventricular tachycardia.

Acknowledgements

This project was partially supported by the "VI Plan Nacional de Investigación Científica, Desarrollo e Innovación Tecnológica" from the Ministerio de Economía y Competitividad of Spain (grant numbers TIN2012-37546-C03-01 and TIN2012-37546-C03-03) and the European Commission (European Regional Development Funds – ERDF – FEDER).

References

[1] E. Carmeliet, Cardiac ionic currents and acute ischemia: from channels to arrhythmias, Physiol. Rev. 79 (3) (1999) 917–1017.

[2] J. Carro, J.F. Rodriguez Matas, V. Monasterio, E. Pueyo, Limitations in electrophysiological model development and validation caused by differences between simulations and experimental protocols, Prog. Biophys. Mol. Biol. (2016), http://dx.doi.org/10.1016/j.pbiomolbio.2016.11.006.
[3] R. Coronel, J.W. Fiolet, F.J. Wilms-Schopman, A.F. Schaapherder, T.A. Johnson, L.S. Gettes, M.J. Janse, Distribution of extracellular potassium and its relation to electrophysiologic changes during acute myocardial ischemia in the isolated perfused porcine heart, Circulation 77 (1988) 1125–1138.
[4] D. Durrer, Th. van Dam, G.E. Freud, M.J. Janse, F.L. Meijler, R.C. Arzbaecher, Total excitation of the isolated human heart, Circulation 41 (1970) 899–912.
[5] S. Dutta, A. Mincholé, E. Zacur, A. Quinn, P. Taggart, B. Rodríguez, Early after depolarizations promote transmural reentry in ischemic human ventricle with reduced repolarization reserve, Prog. Biophys. Mol. Biol. 120 (2016) 236–248.
[6] J.M. Ferrero Jr., J. Saiz, J.M. Ferrero, N.V. Thakor, Simulation of action potentials from metabolically impaired cardiac myocytes: role of ATP-sensitive K^+ current, Circ. Res. 79 (2) (1996) 208–221.
[7] J.M. Ferrero Jr., B. Trenor, B. Rodriguez, J. Saiz, Electrical activity and reentry during acute regional myocardial ischemia: insights from simulations, Int. J. Bifurc. Chaos 13 (2003) 3703–3715.
[8] T. Furukawa, S. Kimura, N. Furukawa, A.L. Bassett, R.J. Myerburg, Role of cardiac ATP-regulated potassium channels in differential responses of endocardial and epicardial cells to ischemia, Circ. Res. 68 (6) (1991) 1693–1702.
[9] D. Geselowitz, W. Miller, A bidomain model for anisotropic cardiac muscle, Ann. Biomed. Eng. 11 (3) (1983) 191–206.
[10] K. Gima, Y. Rudy, Ionic current basis of electrocardiographic waveforms: a model study, Circ. Res. 90 (8) (2002) 889–896.
[11] A.V. Glukhov, V.V. Fedorov, Q. Lou, V.K. Ravikumar, P.W. Kalish, R.B. Schuessler, N. Moazami, I.R. Efimov, Transmural dispersion of depolarization in failing and non failing human ventricle, Circ. Res. 106 (2010) 981–991.
[12] E.A. Heidenreich, J.M. Ferrero, M. Doblaré, J.F. Rodríguez, Adaptive macro finite elements for the numerical solution of monodomain equations in cardiac electrophysiology, Ann. Biomed. Eng. 38 (7) (2010) 2331–2345.
[13] E.A. Heidenreich, J.M. Ferrero, J.F. Rodriguez, Modeling the human heart under acute ischemia, in: B. Calvo, E. Peña (Eds.), Patient-Specific Computational Modeling, Springer, 2012, pp. 81–104.
[14] P.A. Helm, A Novel Technique for Quantifying Variability of Cardiac Anatomy Application to the Dyssynchronous Failing Heart (PhD thesis), Johns Hopkins University, 2005.
[15] M.J. Janse, J. Cinca, H. Morena, J.W. Fiolet, A.G. Kleber, G.P. de-Vries, A.E. Becker, D. Durrer, The "border zone" in myocardial ischemia. An electrophysiological, metabolic, and histochemical correlation in the pig heart, Circ. Res. 44 (4) (1979) 576–588.
[16] M.J. Janse, F.J. van Capelle, H. Morsink, A.G. Kleber, F. Wilms-Schopman, R. Cardinal, C.N. d'Alnoncourt, D. Durrer, Flow of "injury" current and patterns of excitation during early ventricular arrhythmias in acute regional myocardial ischemia in isolated porcine and canine hearts. Evidence for two different arrhythmogenic mechanisms, Circ. Res. 47 (2) (1980) 151–165.
[17] M.J. Janse, A.G. Kleber, Electrophysiological changes and ventricular arrhythmias in the early phase of regional myocardial ischemia, Circ. Res. 49 (1981) 1069–1081.
[18] M.J. Janse, A.G. Kleber, A. Capucci, R. Coronel, F. Wilms-Schopman, Electrophysiological basis for arrhythmias caused by acute ischemia, J. Mol. Cell. Cardiol. 18 (1986) 339–355.
[19] A. Kanai, G. Salama, Optical mapping reveals that repolarization spreads anisotropically and is guided by fiber orientation in guinea-pig hearts, Circ. Res. 77 (1995) 784–802.
[20] S.I. Koumi, R.L. Martin, R. Sato, Alterations in ATP-sensitive potassium channel sensitivity to ATP in failing human hearts, Am. J. Physiol. Heart Circ. Physiol. 272 (4) (1997) 1656–1665.
[21] A. Mena Tobar, J.M. Ferrero, J.F. Rodríguez, GPU accelerated solver for nonlinear reaction-diffusion systems. Application to theelectrophysiology problem, Comput. Phys. Commun. 196 (2015) 280–289.
[22] A. Michailova, W. Lorentz, A. McCulloch, Modeling transmural heterogeneity of KATP current in rabbit ventricular myocytes, Am. J. Physiol. Cell Physiol. 293 (2) (2007) 542–557.
[23] F. Morris, W.J. Brady, ABC of clinical electrocardiography acute myocardial infarction? Part I, BMJ 324 (2002) 831–834.
[24] R. Plonsey, R.C. Barr, Bioelectricity, Plenum, New York, 1989.
[25] B. Rodriguez, B.M. Tice, J.C. Eason, F. Aguel, N. Trayanova, Cardiac vulnerability to electric shocks during phase 1a of acute global ischemia, Heart Rhythm 1 (6) (2004) 695–703.
[26] B. Rodriguez, N. Trayanova, D. Noble, Modeling cardiac ischemia, Ann. N. Y. Acad. Sci. 1080 (2006) 395–414.
[27] M. Rubart, D.P. Zipes, Mechanisms of sudden cardiac death, J. Clin. Invest. 115 (9) (2005) 2305–2315.
[28] W.T. Smith, W.F. Fleet, T.A. Johnson, C.L. Engle, W.E. Cascio, The Ib phase of ventricular arrhythmias in ischemic in situ porcine heart is related to changes in cell-to-cell electrical coupling, Circulation 92 (1995) 3051–3060.
[29] P. Taggart, P.M.I. Sutton, T. Opthof, R. Coronel, R. Trimlett, W. Pugsley, P. Kallis, Inhomogeneous transmural conduction during early ischemia in patients with coronary artery disease, J. Mol. Cell. Cardiol. 32 (2000) 621–639.
[30] K.H.W.J. ten Tusscher, A.V. Panfilov, Alternans and spiral breakup in a human ventricular tissue model, Am. J. Physiol. Heart Circ. Physiol. 291 (3) (2006) 1088–1100.
[31] R.S. MacLeod, C.R. Johnson, P.R. Ershler, Construction of an inhomogeneous model of the human torso for use in computational electrocardiography, in: Proceedings of the 13th Annual International Conference of the IEEE Engineering in Medicine and Biology Society, Orlando, FL, USA, 1991, pp. 688–689.
[32] B. Tice, B. Rodriguez, N. Trayanova, Arrhythmogenicity of transmural heterogeneities in a realistic model of regional ischemia, Heart Rhythm 2 (5) (2005) S261.
[33] D.L. Weiss, M. Ifland, F.B. Sachse, G. Seemann, O. Dossel, Modeling of cardiac ischemia in human myocytes and tissue including spatiotemporal electrophysiological variations, Biomed. Tech. 54 (3) (2009) 107–125.
[34] R.L. Wilensky, J. Tranum-Jensen, R. Coronel, A.A.M. Wilde, J.W.T. Fiolet, M.J. Janse, The subendocardial border zone during acute ischemia of the rabbit heart: an electrophysiologic, metabolic, and morphologic correlative study, Circulation 74 (1986) 1137–1146.
[35] A. Yatani, A.M. Brown, N. Akaike, Effect of extracellular ph on sodium current in isolated, single rat ventricular cells, J. Membr. Biol. 78 (2) (1984) 163–168.

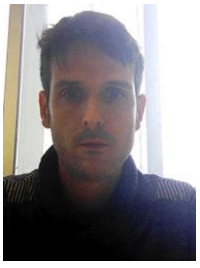

Andrés Mena Tobar was born in Zaragoza (Spain) in 1977. He received his degree in Computer Science Engineering in 2003, and a MSc in Biomedical Engineering in 2012, being currently a PhD candidate in the PhD program in Biomedical Engineering at the University of Zaragoza in the development of a monodomain solver in GPU for electrophysiology applications. He works as a researcher at CIBER-BBN since 2012. Has co-author eight journal publications and participated in six international conferences.

José M. Ferrero was born in Madrid (Spain) in 1966. He received his Electrical and Electronic Engineering Degree in 1990. In 1995, after serving as a research trainee in the Department of Biomedical Engineering of the Johns Hopkins University (Baltimore, USA), he obtained his PhD degree in Biomedical Engineering from the Universidad Politecnica de Valencia (Spain), where he is now Full Professor. He teaches and conducts research in bioelectricity and computational simulation of cardiac electrophysiology.

Francesco Migliavacca obtained a MSc in Mechanical Engineering in 1992 and a PhD in Bioengineering in 1997 both from Politecnico di Milano. In 2000 he worked as a Research Assistant at the Cardiothoracic Unit of Great Ormond Street Hospital for Children in London in 1994 and 1997–99. In 2000 and 2001 he was consultant and Research Scientist at the Pediatric Cardiac Surgery Department of the University of Michigan, Ann Arbor, MI, USA. At present he is a Full Professor of Bioengineering in the Department of Chemistry, Materials and Chemical Engineering Giulio Natta of Politecnico di Milano. He is involved in funded researches from the European Commission, the Foundation Leducq and public and private Italian National programs. He received the medal Le Scienze 2001 in Engineering and was awarded the European Society of Biomechanics Perren Award in 2004. He is Associate Editor of the peer-reviewed journals Cardiovascular Engineering and Technology and Frontiers in Pediatric Cardiology.

José F. Rodríguez Matas received the B.E. degree in mechanical engineering from Universidad Sim-nBol'var, Caracas, Venezuela in 1993, and the Ph.D. degree in mechanical engineering from the University of Notre Dame, IN, in 1999. He is currently an Associate Professor of bioengineering in the Department of Chemistry, Materials and Chemical Engineering Giulio Natta at Politecnico di Milano. His research interests concern computational mechanics applied to the biomechanics of soft tissues and couple biophysical problems. He is particularly involved in nonlinear finite element applications, and the development of efficient computational tools for cardiac electrophysiology and couple problems.